ISSN 2229-5518

Nonlinear behavior investigation of zyncite-iron semiconductor junction

Michał Nowicki, Roman Szewczyk

Abstract— In this paper, we present the investigation of zyncite-iron semiconductor junction voltage-current characteristics. They were measured on the special measurement stand, in the octopus, or curve-tracer pattern. Nonlinear behavior, such as hysteresis, S-type negative dynamic resistance, and memristance-like behavior, were observed. The test stand is especially convenient to use for students, on electronics/material science classes.

Index Terms— ZnO, Zyncite, hysteresis, memristance

---

1 Introduction

THE zinc oxide, with its unique physical and chemical properties, such as high chemical stability, high electrochemical coupling coefficient, broad range of radiation absorption and high photostability, is a truly multifunctional, or 'smart' material. The piezo- and pyroelectric properties of ZnO mean that it can be used as a sensor, converter, energy generator and photocatalyst in hydrogen production. In materials science, zinc oxide is classified as a semiconductor in group II-VI, whose covalence is on the boundary between ionic and covalent semiconductors. A broad energy band (3.37 eV), high bond energy (60 meV) and high thermal and mechanical stability at room temperature make it attractive for potential use in electronics, optoelectronics and laser technology. Because of its hardness, rigidity and piezoelectric constant it is an important material in the ceramics industry, while its low toxicity, biocompatibility and biodegradability make it a material of interest for biomedicine and in pro-ecological systems [1,2].

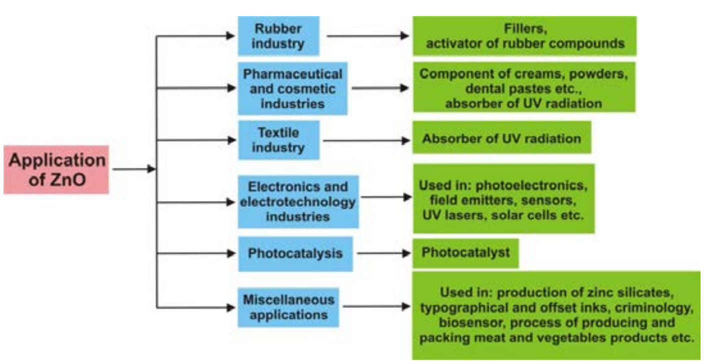

Fig. 1. ZnO applications [1]

The crystallized form of ZnO is called the zyncite. Its crystal form is rare in nature; a known exception to this is at the Franklin and Sterling Hill Mines in New Jersey, USA. It has a hexagonal crystal structure, and a color that depends on the presence of impurities. The zincite found at Franklin Furnace is red-colored (mostly due to iron and manganese) and associated with willemite and franklinite.

Zincite crystals can be grown artificially, and synthetic zincite crystals are available as a unwanted by-product of zinc smelting. Synthetic crystals can be colorless or can range in color from dark red, orange, or yellow to light green.

TABLE 1
ZYNCITE PHYSICAL PROPERTIES

Property	Description/Value
Crystal habit	Disseminated – occurs in small, distinct particles dispersed in matrix.
Crystal system	Hexagonal dihexagonal pyramidal 6mm
Twinning	On {0001}
Cleavage	On {1010}, perfect; parting on {0001}
Fracture	Conchoidal
Tenacity	Brittle
Mohs scale hardness	4
Luster	Subadamantine to resinous
Streak	Yellowish orange
Diaphaneity	Translucent, transparent in thin fragments
Specific gravity	5.64–5.68
Optical properties	Uniaxial (+)
Refractive index	$n\omega = 2.013$, $n\varepsilon = 2.029$
Birefringence	$\delta = 0.016$

Nonlinear electric behavior of the Zyncite crystal were heavily investigated by O. Lossev, and he was the first to utilize it in active amplification devices [3]. Today, the extraordinary behavior of these semiconductors may prove useful in high-frequency applications, such as generators, and other emerging technologies [4-9].

• *Michal Nowicki* is with Industrial Research Institute for Automation and Measurements, Jerozolimskie 202, 02-486 Warsaw, Poland*
nowicki@mchtr.pw.edu.pl
• *Roman Szewczyk is with Institute of Metrology and Biomedical Engineering, Warsaw University of Technology, Boboli 8, 02-525 Warsaw, Poland*
r.szewczyk@mchtr.pw.edu.pl,

ISSN 2229-5518

2 MEASUREMENT STAND

The voltage–current characteristics of the zyncite-iron semiconductor junction were measured on the octopus-type measurement circuit. The schematic diagram of the circuit is presented on Figure 2. First, the AC signal of selectable frequency and amplitude is generated by the power output of the universal signal generator. It is then fed through the separator transformer, to cut off any DC bias, and provide isolation from the mains. The induced AC voltage is then applied to the two-terminal device under test, and 100 Ohm calibrated resistor connected in series. Voltage measured across the tested device is measured by the X oscilloscope input, and voltage across the resistor, proportional to the current in the circuit, is measured by the Y scope input. The oscilloscope used may be analogue type, for ease of operation and robustness, or digital, which allow for signal acquisition. Two-terminal test device is presented on Figure 3, it is a variation of the cats-whisker detector. The Zyncite crystals used in this investigation were obtained from the zinc-smelting plant in Poland, and have the visible red hue due to the iron impurities.

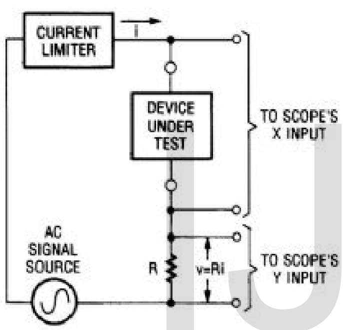

Fig. 2. Voltage-current characteristics tester schematic diagram

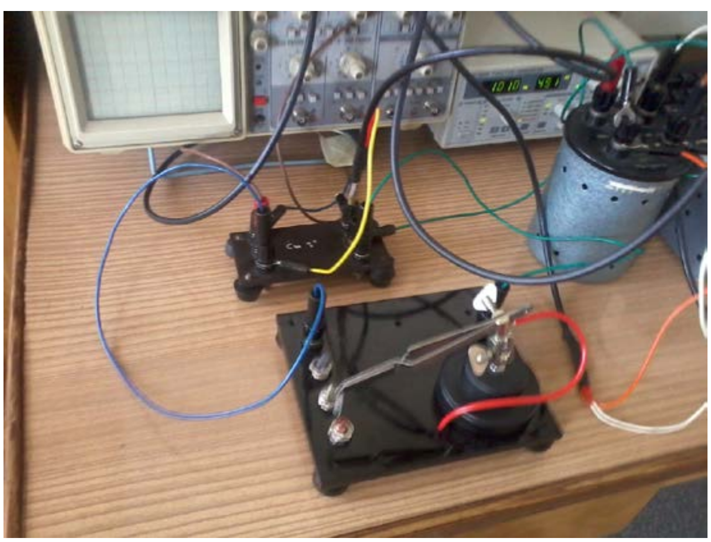

Fig. 3. Measurement stand photo. Two-terminal test device visible in the front.

3 MEASUREMENT RESULTS

On the figures below one can see the nonlinear behavior of the zyncite-iron semiconductor. On the Figures 4-12 the voltage–current characteristics of 9 investigated samples are presented. The AC signal applied was 50 V_{pp} in amplitude, and of 100Hz frequency. Most of the results are similar to the triac, or double diode, operation. The Figures 8,9 and 11 show the unusual, hysteretic characteristics, with area of S-type negative dynamic resistance. Figures 13-15 show the sample 10 response to change of the operating frequency. At 10 Hz there is no hysteresis, and very distinct S-type resistance area. At 100 Hz it behaves like triac, and at 1kHz the voltage-current characteristic is similar to that of the memristor. The memristive effect is unfortunately a function of the operating frequency, and thus shouldn't be considered as such a device. Although it could be used in specific-frequency applications.

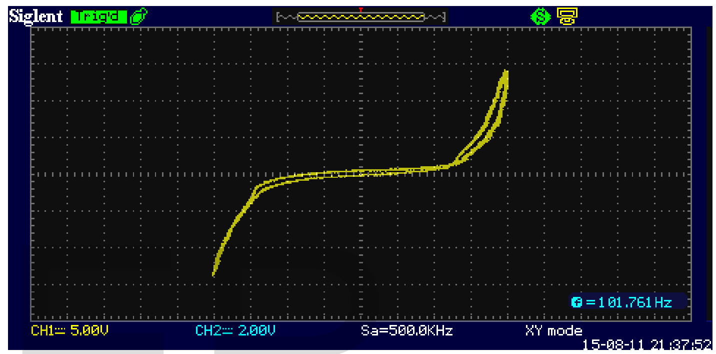

Fig. 4. Measurement results, sample 1

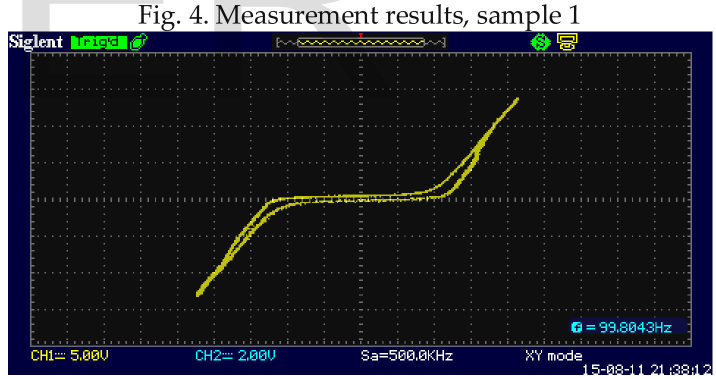

Fig. 5. Measurement results, sample 2

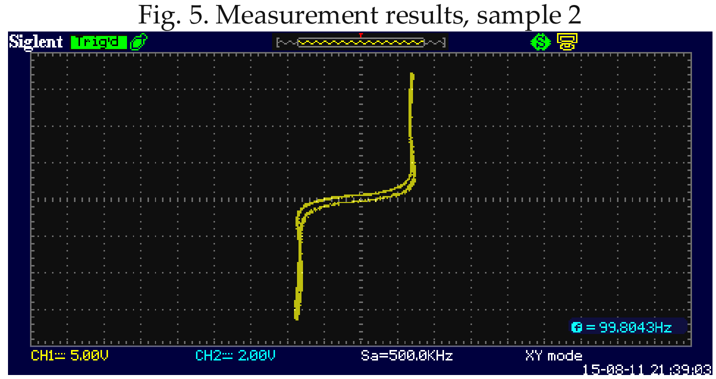

Fig. 6. Measurement results, sample 3

ISSN 2229-5518

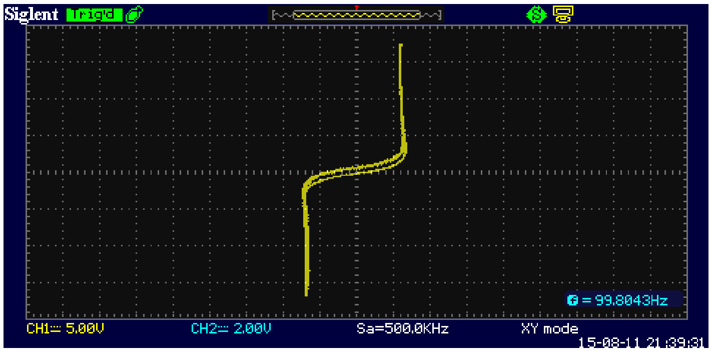

Fig. 7. Measurement results, sample 4

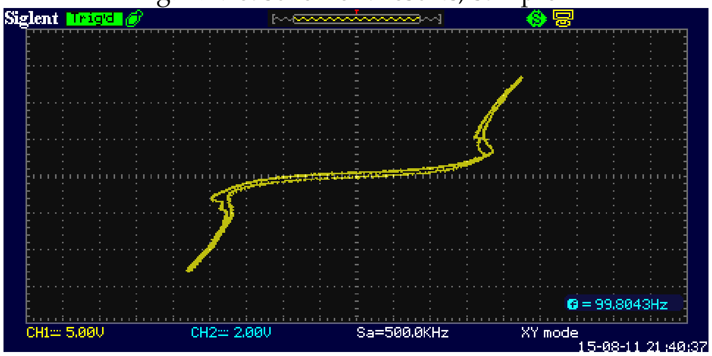

Fig. 8. Measurement results, sample 5. Visible hysteresis, and S-type negative dynamic resistance.

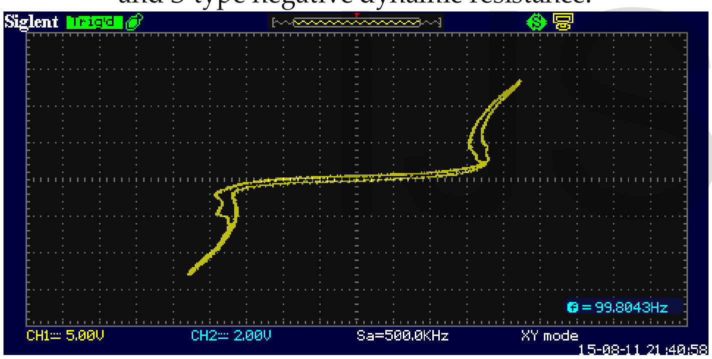

Fig. 9. Measurement results, sample 6. Visible hysteresis, and S-type negative dynamic resistance.

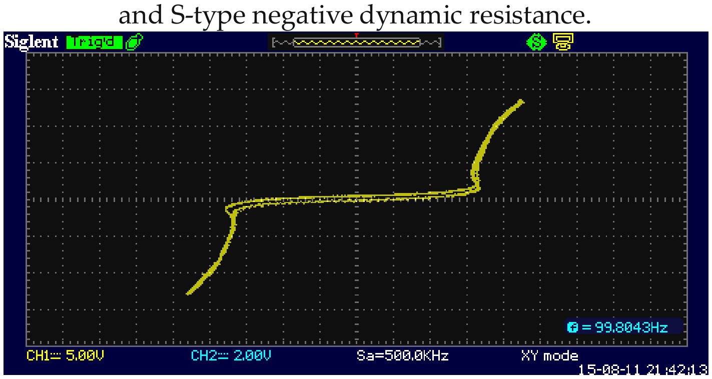

Fig. 10. Measurement results, sample 7. Visible S-type negative dynamic resistance area.

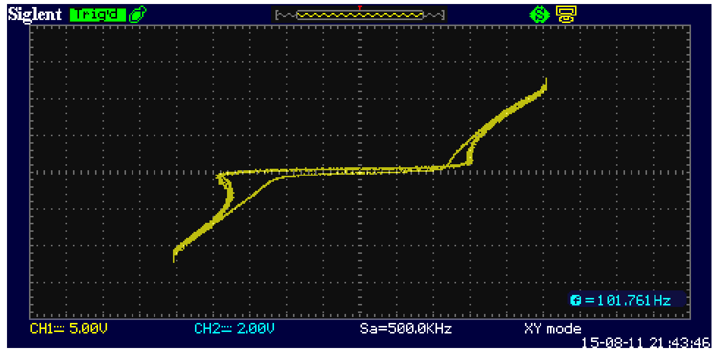

Fig. 11. Measurement results, sample 8. Visible hysteresis, and S-type negative dynamic resistance.

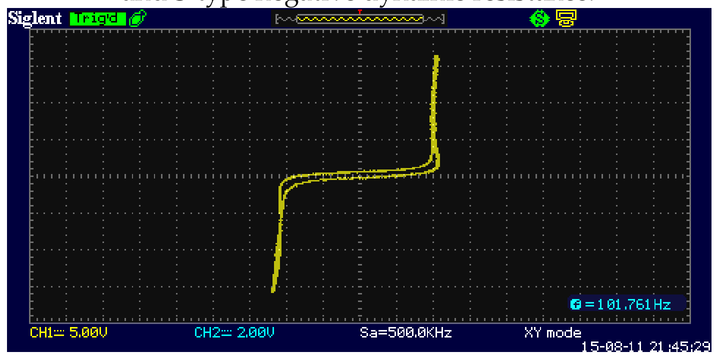

Fig. 12. Measurement results, sample 9

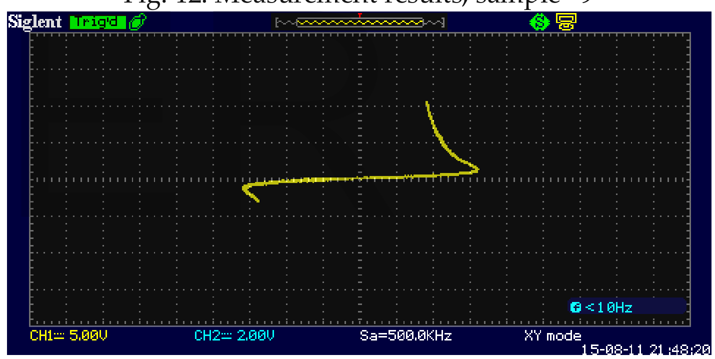

Fig. 13. Measurement results, sample 10. Applied signal frequency: 10 Hz. Very distinct S-type negative dynamic resistance area, and visible lack of symmetry.

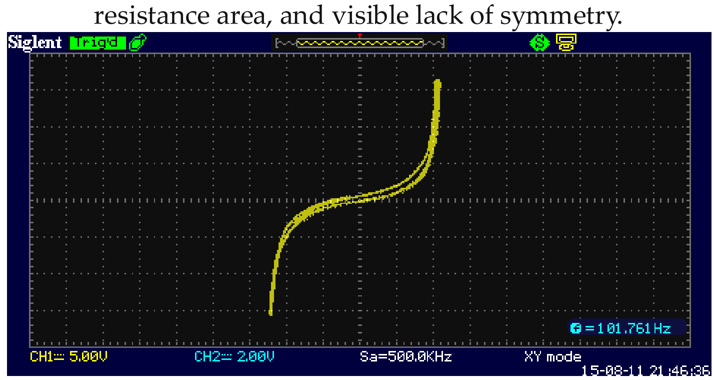

Fig. 14. Measurement results, sample 10. Applied signal frequency: 100 Hz. Triac-like mode of operation.

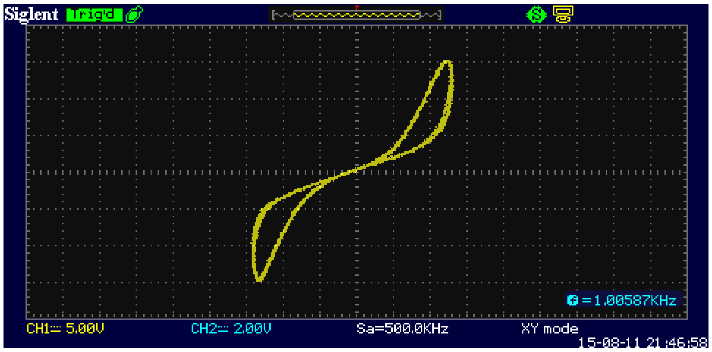

Fig. 15. Measurement results, sample 10. Applied signal frequency: 1000 Hz. Visible 'butterfly', or pinched, hysteresis, typical for memristive devices.

4 Conclusions

The measurement stand for real-time voltage-current characteristics of two-terminal devices was designed and built. The experimental zyncite-iron semiconductor junctions were prepared, and their characteristics presented. Some of the samples are notable for hysteretic behavior, other for distinct S-type negative resistance area. The differences are due to the random orientation of the crystal structure in the junction point-of-contact.

It was shown, that the nonlinearity of the devices response is a function of the operating frequency, and changes dramatically. For 10 Hz it may operate like s-type tunnel diode, for 100 Hz like triac, and for 1 kHz it is similar to memristor.

The proposed methodology is especially convenient for students, during the classes on functional materials or semiconductors. The measurement stand may be used for other two terminal devices as well, such as resistors, diodes, inductors and capacitors, presenting their respective I(V) curves in real-time.

References

[1] Kołodziejczak-Radzimska A., Jesionowski T: Zinc Oxide—From Synthesis to Application: A Review, Materials 2014, 7(4), 2833-2881;

[2] Özgür, Ü.; Alivov, Y.I.; Liu, C.; Teke, A.; Reshchikov, M.A.; Dođan, S.; Avrutin, V.; Cho, S.J.; Morkoç, H. A comprehensive review of ZnO materials and devices. J. Appl. Phys 2005, 98.

[3] Gabel V., The crystal a a generator and amplifier, The Wireless World And Radio Review, 1924, pp 2-5, 47-50

[4] Segets, D.; Gradl, J.; Taylor, R.K.; Vassilev, V.; Peukert, W. Analysis of optical absorbance spectra for the determination of ZnO nanoparticle size distribution, solubility, and surface energy. ACS Nano 2009, 3, 1703–1710.

[5] Lou, X. Development of ZnO series ceramic semiconductor gas sensors. J. Sens. Trans. Technol 1991, 3, 1–5.

[6] Bacaksiz, E.; Parlak, M.; Tomakin, M.; Özcelik, A.; Karakiz, M.; Altunbas, M. The effect of zinc nitrate, zinc acetate and zinc chloride precursors on investigation of structural and optical properties of ZnO thin films. J. Alloy. Compd 2008, 466, 447–450.

[7] Wang, J.; Cao, J.; Fang, B.; Lu, P.; Deng, S.; Wang, H. Synthesis and characterization of multipod, flower-like, and shuttle-like ZnO frameworks in ionic liquids. Mater. Lett 2005, 59, 1405–1408.

[8] Wang, Z.L. Splendid one-dimensional nanostructures of zinc oxide: A new nanomaterial family for nanotechnology. ACS Nano 2008, 2, 1987–1992

[9] Chaari, M.; Matoussi, A. Electrical conduction and dielectric studies of ZnO pellets. Phys. B Condens. Matter 2012, 407, 3441–3447.